Essential role for proteinase-activated receptor-2 in arthritis

See the related Commentary beginning on page 25.

William R. Ferrell,[1] John C. Lockhart,[2] Elizabeth B. Kelso,[1] Lynette Dunning,[2] Robin Plevin,[3] Stephen E. Meek,[4] Andrew J.H. Smith,[4] Gary D. Hunter,[3] John S. McLean,[2] Frances McGarry,[2] Robert Ramage,[5] Lu Jiang,[5] Toru Kanke,[6] and Junichi Kawagoe[6]

[1]Centre for Rheumatic Diseases, Royal Infirmary, University of Glasgow, Glasgow, United Kingdom
[2]Department of Biological Sciences, University of Paisley, Paisley, United Kingdom
[3]Department of Physiology & Pharmacology, University of Strathclyde, Glasgow, United Kingdom
[4]Gene Targeting Laboratory, Centre for Genome Research, University of Edinburgh, Edinburgh, United Kingdom
[5]Albachem Limited, Elvingston Science Centre, East Lothian, United Kingdom
[6]Tokyo New Drug Research Laboratories, Pharmaceutical Division, Kowa Company Limited, Tokyo, Japan

Using physiological, pharmacological, and gene disruption approaches, we demonstrate that proteinase-activated receptor-2 (PAR-2) plays a pivotal role in mediating chronic inflammation. Using an adjuvant monoarthritis model of chronic inflammation, joint swelling was substantially inhibited in PAR-2–deficient mice, being reduced by more than fourfold compared with wild-type mice, with virtually no histological evidence of joint damage. Mice heterozygous for *PAR-2* gene disruption showed an intermediate phenotype. PAR-2 expression, normally limited to endothelial cells in small arterioles, was substantially upregulated 2 weeks after induction of inflammation, both in synovium and in other periarticular tissues. PAR-2 agonists showed potent proinflammatory effects as intra-articular injection of ASKH95, a novel synthetic PAR-2 agonist, induced prolonged joint swelling and synovial hyperemia. Given the absence of the chronic inflammatory response in the PAR-2–deficient mice, our findings demonstrate a key role for PAR-2 in mediating chronic inflammation, thereby identifying a novel and important therapeutic target for the management of chronic inflammatory diseases such as rheumatoid arthritis.

J. Clin. Invest. **111**:35–41 (2003). doi:10.1172/JCI200316913.

Introduction

In recent years there has been increasing interest in proteinase-activated receptor-2 (PAR-2) as a mediator of neurogenic inflammation (1) and nociception (2). The rapid induction of PAR-2 in blood vessels following injury (3) points to a potential role in mediating non-neurogenic inflammatory responses. As a G protein–coupled receptor that is rapidly desensitized following activation, PAR-2 is generally considered to mediate only acute inflammatory responses, and studies performed to date have examined only the effect of administration of PAR-2 agonists over a short time (up to 6 hours). Although important in injury responses, acute inflammation is relatively short-lived and seldom requires medical intervention. By contrast, chronic inflammatory responses, typified by debilitating conditions such as rheumatoid arthritis, are rarely self-limiting and present a greater medical challenge. An important question we wished to address is whether PAR-2 mediates chronic inflammatory processes. We tested this hypothesis by inducing a chronic model of arthritis (a classic example of chronic inflammatory disease) in PAR-2–deficient mice. Our results demonstrate that disruption of the *PAR-2* gene results in ablation of chronic arthritis and that PAR-2 is greatly upregulated in inflamed tissues, providing strong evidence for a key role of PAR-2 in mediating chronic inflammation.

Received for publication September 16, 2002, and accepted in revised form October 29, 2002.

Address correspondence to: William R. Ferrell, Centre for Rheumatic Diseases, Royal Infirmary, 10 Alexandra Parade, Glasgow G31 2ER, United Kingdom. Phone: 44-141-211-4688; Fax: 44-141-211-0414; E-mail: w.ferrell@bio.gla.ac.uk.

Conflict of interest: The authors have declared that no conflict of interest exists.

Nonstandard abbreviations used: proteinase-activated receptor-2 (PAR-2).

Methods

Generation of PAR-2–deficient mice. Homologous recombination in ES cells was used to create a null allele of the PAR-2 gene, which also incorporated a β-galactosidase reporter gene. A 129/Ola mouse genomic λ 2001 library was screened with a PAR-2 cDNA probe to isolate cloned DNA for the targeting vector construction. The targeting vector consisted of a total of approximately 9 kb of cloned genomic DNA sequence, which flanked both sides of exon 2 (Figure 1a). An 813-nucleotide internal region of exon 2 contained as a *Cla*I-*Sal*I restriction fragment was removed and replaced with the reporter/selection cassette TAG3/IRES/*lacZ*pA/MC1*neo*pA (4). E14Tg2a ES cells cultured according to standard protocol (5) were electroporated with *Not*I-linearized targeting vector and selected in G418. G418-resistant ES cell clones

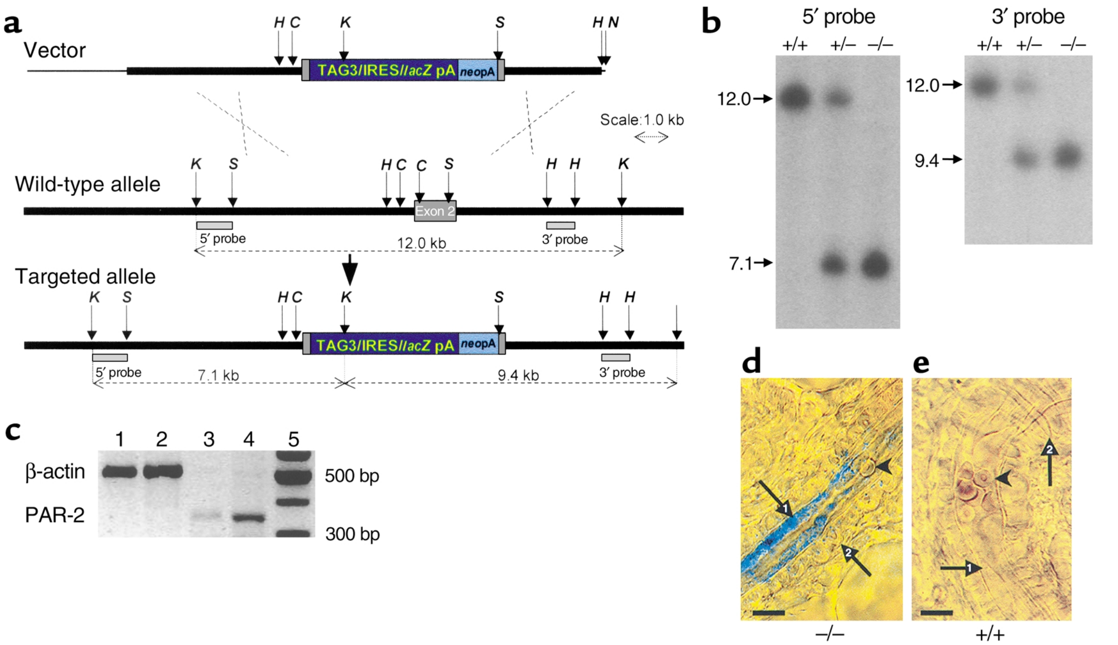

Figure 1

Generation of PAR-2–deficient mice. (**a**) Structure of the PAR-2 targeting vector (top), the wild-type *PAR-2* allele (middle), and targeted allele (bottom) resulting from replacement recombination at the dashed crosses. The null allele was created by substitution of a reporter/selection cassette (dark and light blue boxes) for most of the exon 2 sequence (filled gray box). Non-exon–containing chromosomal and cloned genomic DNA sequence is shown by a thick black line and pBluescript plasmid sequence by a thin black line. Restriction enzyme sites *Cla*I (*C*), *Hin*dIII (*H*), *Kpn*I (*K*), *Not*I (*N*), and *Sal*I (*S*) are indicated by small arrows, and the sizes of relevant restriction fragments are shown by dotted lines. The targeted allele was identified by *Kpn*I digestion and hybridization with the 5′ and 3′ flanking probe fragments (gray rectangles). (**b**) Southern blot analysis of *Kpn*I-digested genomic DNA prepared from pups from an intercross mating of PAR-2 mice heterozygous (+/–) for the null allele, demonstrating the presence of viable mice homozygous for the null allele (–/–). (**c**) RT-PCR for β-actin (548 bp) and PAR-2 (380 bp) mRNA expression in articular (lane 1 and lane 3, respectively) and intestinal (positive control; lane 2 and lane 4, respectively) tissue from *PAR-2*$^{+/+}$ mice. (**d**) High-power view (oil immersion, differential interference contrast) of a synovial arteriole from a *PAR-2*$^{-/-}$ mouse. (**e**) Synovial tissue from a *PAR-2*$^{+/+}$ mouse. β-galactosidase activity absent in endothelial cells (arrow 1) from *PAR-2*$^{+/+}$ mice compared with *PAR-2*$^{-/-}$ tissue. Erythrocytes (arrowheads) are clearly visible in the lumen as are surrounding smooth muscle cells (arrow 2). Scale bar: 10 μm.

were screened by Southern blot analysis of *Kpn*I-digested ES cell clone DNAs using hybridization probes flanking and external to the vector homology arm sequences (Figure 1a) and targeted clones were detected at a frequency of approximately 9%. Targeted ES cells were injected into C57BL/6 blastocysts to generate chimeras according to standard protocol (6). The resulting male chimeras were subsequently test crossed with C57BL/6 females, and germline transmission was confirmed in agouti coat colored test-cross offspring by Southern blot analysis of *Kpn*I-digested DNA obtained from tail biopsy (Figure 1b). Male and female test-cross offspring heterozygous for the null allele (*PAR-2*$^{+/-}$) were intercrossed to generate homozygous (*PAR-2*$^{-/-}$) mice. *PAR-2*$^{-/-}$ mice were obtained at a normal mendelian ratio and were phenotypically similar to *PAR-2*$^{+/+}$ and *PAR-2*$^{+/-}$ littermates, exhibiting no macroscopic evidence of any abnormalities. The PAR-2–deficient strain was maintained by backcrossing heterozygous males with C57BL/6 females (Harland UK Ltd., Loughborough, United Kingdom) at each generation. Heterozygous mice at backcross generations three and four were used to set up intercrosses to generate the homozygous, heterozygous, and wild-type littermates used in the experimental analyses described herein. All experimentation was in accordance with the Animals (Scientific Procedures) Act 1986 of the United Kingdom.

Analysis of PAR-2 expression. Direct evidence for PAR-2 expression in the mouse knee was obtained by RT-PCR performed on synovial tissue harvested from *PAR-2*$^{+/+}$ mice and compared with intestine, which was used as a positive control (Figure 1c). Total cellular RNA was extracted from tissue using TRIzol reagent (Invitrogen Ltd., Paisley, United Kingdom). RT-PCR was performed using the Reverse Transcription System from Promega UK (Southhampton, United Kingdom). Aliquots (2 μl) of cDNA were used as templates for amplification by PCR using ReddyMix (Abgene, Ashford, United Kingdom) and the following intron spanning PAR-2 primers 5′-ATGCGAAGTCTCAGCCTGGCG-3′ and 5′-GAGAGGAGGTCGGCCAAGGCC-3′ to yield a 380-bp PCR product. The signal yielded by the PAR-2 primer pair was normalized to the PCR product generated by an intron spanning actin primer pair 5′-GTGGGGCGCCCCAGGCACCA-3′ and 5′-CTCCTTAATGTCACGCACGATTTC-3′ (548 bp). Thermal cycling was performed under the correct conditions for PCR detection of PAR-2 (7).

PCR products were separated on a 1.5% agarose gel and visualized by ethidium bromide staining. The PAR-2 PCR product was excised from the gel and purified using the Concert Gel Extraction System (Invitrogen Ltd.), and its identity was confirmed by sequencing with the BigDye Terminator method using an ABI 3100 automated sequencer (Applied Biosystems, Warrington, United Kingdom) and compared with published data. In addition, in the targeting vector designed for disruption of the *PAR-2* gene, the sequence of the β-galactosidase gene is preceded by an internal ribosome entry site sequence (8) embedded in the exon sequence. Consequently, a bicistronic transcription unit is generated in which expression of β-galactosidase is brought under control of PAR-2 transcriptional regulatory elements. Thus staining for β-galactosidase activity can be used to monitor expression of the targeted *PAR-2* allele. This was achieved by incubating synovial tissues for 24 hours with X-gal (5-bromo-4-chloro-3-indolyl-β-D-galactopyranoside; Sigma-Aldrich, Poole, United Kingdom), a substrate of β-galactosidase that yields a blue chromophore when cleaved by the enzyme. The tissues were then examined for staining by light microscopy, which revealed reaction product in the endothelium of synovial blood vessels from *PAR-2*$^{-/-}$ mice but a complete absence of staining in *PAR-2*$^{+/+}$ mice (Figure 1, d and e). Images are contrast-enhanced and color balance optimized.

PAR-2 agonists. PAR-2 agonists used were SLIGRL-NH_2 (Tocris Cookson Ltd., Avonmouth, United Kingdom) and ASKH95 (2-furoyl-LIGKV-OH; Figure 2). Due to the technical difficulty in synthesizing the reverse sequence peptide to ASKH95, a structurally similar peptide, ASKH115 (phenylacetyl-LIGKV-OH; Figure 2), was used as the control peptide. Acetylation of the amino terminus of PAR-2 agonists has previously been shown to eliminate their ability to activate PAR-2 (9, 10). Furthermore, our own data in NCTC2544 cells, which stably express human PAR-2 (11), indicate that ASKH95 has an effective concentration for a 50% response (EC_{50}) of 8.3 μM in an inositol turnover assay (12), whereas ASKH115 shows no PAR-2 activity up to 1 mM. Activation of PAR-2 by the agonists SLIGRL and SLIGKV is evidenced by their mobilization of intracellular Ca^{2+} (10). We find that ASKH95 induces Ca^{2+} signaling in NCTC2544 cells stably expressing human PAR-2 but not in control cells (data not shown). ASKH95 and ASKH115 were synthesized on an ABI 430 peptide synthesizer (Applied Biosystems) using Fmoc chemistry (13). The side-chain protection groups were Ser(tBu) and Lys(Boc). HOCt/DIC were used as coupling reagents. All non-amino acids were coupled through their acid chloride. The crude peptide was cleaved from the resin and purified by HPLC (Gilson International France SAS, Villiers-le-Bel, France). The vehicle for the peptides was 0.9% NaCl.

Induction of inflammation. Chronic arthritis was induced by injection of Freund's complete adjuvant (10 mg/ml heat-killed *Mycobacterium tuberculosis*): 20 μl into the joint space and periarticular injection of 80 μl, equally divided among four sites, under general anesthesia (O_2/N_2O/2% halothane) after prior measurement of knee joint diameter. Joint swelling was assessed by measuring knee joint diameter using spring-loaded calipers (Kroeplin GmbH, Schluechtern, Germany).

Acute joint inflammation was induced by intra-articular injection of 20 μl 2% λ carrageenan and 1% kaolin (Sigma-Aldrich) in sterile 0.9% saline under general anesthesia, which was then discontinued. Measurements of knee joint diameter were taken 24 hours later. The untreated contralateral knee was also measured at the same timepoint. In four animals, one knee was injected with sterile vehicle as a control. Repeated measurements of normal knees on five successive days were reproducible (coefficient of variation, 2%).

Blood flow measurements. Synovial perfusion was assessed by laser Doppler imaging (Perimed AB, Stockholm, Sweden) of the exposed medial aspect of the mouse knee joint capsule, a method we have previously validated and used extensively (14). This involved scanning a low-power (1 mW) laser (635 nm) across the exposed external surface of the medial aspect of the knee joint. Drugs (100 μl) were applied topically to the capsule. Blood pressure was monitored by cannulation of the carotid artery.

Histological assessment of arthritis. Knee joints were fixed in 10% neutral formal saline and then decalcified in 5% nitric acid for 72 hours, and 6-μm paraffin sections were prepared. These were stained with hematoxylin, safranin O, and fast green and evaluated by two observers blinded to animal genotype and treatment. The severity of arthritic changes, in terms of cellular infiltrate, synovial hyperplasia, and cartilage damage, was scored on a 0–3 scale for each and a total score was calculated. Maximum possible score per animal was 9. The scores from the two observers were in close agreement and were therefore averaged.

ASKH115

ASKH95

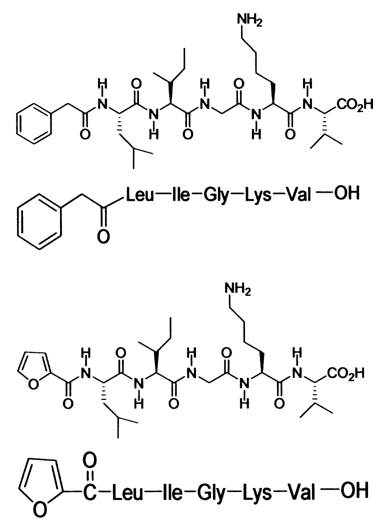

Figure 2
Structure of the synthetic peptides ASKH95 (PAR-2 agonist) and ASKH115 (PAR-2 inactive).

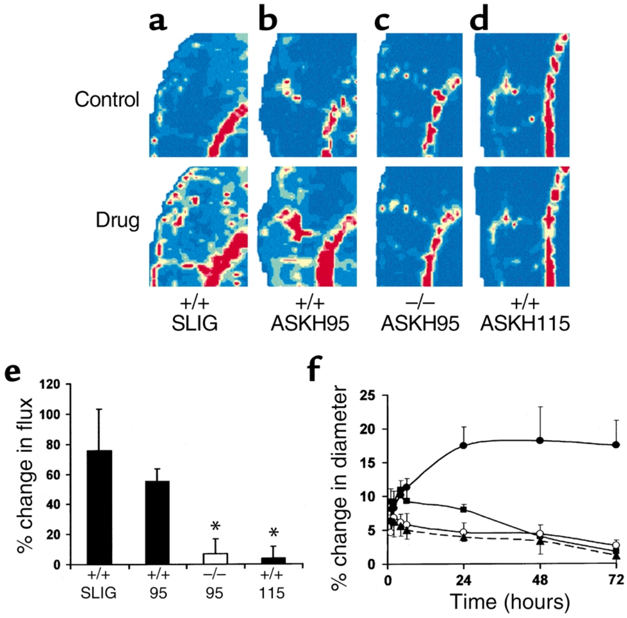

Figure 3
Effects of PAR-2 agonists on synovial perfusion and joint swelling. (**a**) Laser Doppler image showing vasodilatation 1 minute after topical administration of 1 μg of the PAR-2 agonist SLIGRL-NH_2 (SLIG) to *PAR-2*$^{+/+}$ mice. (**b**) ASKH95 (1 μg) administered to *PAR-2*$^{+/+}$ mice also elicits vasodilatation. (**c**) ASKH95 (1 μg) administered to *PAR-2*$^{-/-}$ mice is without effect. (**d**) The control peptide ASKH115 (1 μg) administered to *PAR-2*$^{+/+}$ mice is without effect. (**e**) Histogram showing quantitative data for the vasodilator effect of SLIG in *PAR-2*$^{+/+}$ mice (+/+ SLIG), ASKH95 in both *PAR-2*$^{-/-}$ mice (–/– 95) and wild-type mice (+/+ 95), and ASKH115 in wild-type mice (+/+ 115). Perfusion is measured in arbitrary "flux units" and color coded in the images, with dark blue being the lowest and dark red the highest. Data are presented as mean ± SEM. n = 5–7. *P < 0.01 compared with +/+ 95. (**f**) Intra-articular injection of 100 μg of SLIG in *PAR-2*$^{+/+}$ mice (filled squares) elicits an increase in joint diameter that reaches a maximum within 4 hours but declines thereafter. The synthetic PAR-2 agonist ASKH95 (100 μg) produces joint swelling that reaches maximum by 24 hours and is sustained thereafter in *PAR-2*$^{+/+}$ mice (filled circles), a response that differs significantly compared with the same dose of this peptide in *PAR-2*$^{-/-}$ mice (open circles) and control peptide ASKH115 in wild-type mice (filled triangles). Data are presented as mean ± SEM; n = 4–10.

Statistical analysis. Data are expressed as mean ± SEM and comparisons were performed using the two-tailed Student t test or one- or two-way ANOVA as appropriate.

Results

Activation of PAR-2 in the knee joint using the native peptide SLIGRL-NH_2 or ASKH95, a synthetic PAR-2 agonist, resulted in joint swelling and hyperemia, well-recognized indices of inflammation. Topical administration of SLIGRL-NH_2 (1 μg) to the exposed joint capsule in *PAR-2*$^{+/+}$ mice elicited vasodilatation at the 1-minute timepoint (Figure 3a). The same dose of ASKH95 given to *PAR-2*$^{+/+}$ mice produced vasodilatation that was sustained for more than 5 minutes (Figure 3b), but negligible change in *PAR-2*$^{-/-}$ mice (Figure 3c), confirming the specificity of this novel agonist for PAR-2. This is supported by the lack of effect of ASKH115, the control peptide for ASKH95, in *PAR-2*$^{+/+}$ mice (Figure 3, d and e). Furthermore, synovial vasodilatation in response to ASKH95 (1 μg) was unaffected by coadministration of ASKH115 (5 μg), demonstrating no antagonistic activity of the latter (data not shown). Consistent with the work of Damiano and colleagues (15), higher doses of the PAR-2 agonists elicited depressor responses in *PAR-2*$^{+/+}$ mice, thus complicating measurement of joint perfusion. In contrast, administration of ASKH95 had no effect on blood pressure in *PAR-2*$^{-/-}$ mice, even at a dose of 100 μg, further confirming that the effects of this agonist are mediated through PAR-2.

Following a single intra-articular injection of ASKH95, joint diameter increased substantially in wild-type mice, reaching maximum by 24 hours. Unexpectedly, this increase was sustained for up to 72 hours (Figure 3f). SLIGRL-NH_2 also produced joint swelling, although with a more rapid onset and shorter duration. ASKH115 failed to elicit significant joint swelling. Injection of ASKH95 into the knee joint of *PAR-2*$^{-/-}$ mice resulted in a response that was significantly lower than that seen in wild-type mice (P < 0.0001, two-way ANOVA), but was not significantly different from that following intra-articular injection of ASKH115 (Figure 3f), pharmacologically confirming the absence of PAR-2. The prolonged time course over which ASKH95 mediates swelling is substantially longer than that observed in previous studies where maximum paw swelling was reached within 1–2 hours, but had declined by 6 hours (1, 2). This may be related to differences in the compounds used, but differences could also have arisen from the site of injection (knee joint versus paw) or been due to the species (mouse versus rat).

The observation that a single dose of ASKH95 leads to prolonged joint swelling suggests that persistent endogenous activation of PAR-2 could play a pivotal role in chronic joint inflammation. This was further investigated in a murine model of chronic arthritis. Combined intra- and periarticular administration of Freund's complete adjuvant produced a substantial increase in knee joint diameter, characterized by a rapid initial increase within 24 hours followed by a more progressive rise, reaching a plateau by 2–3 weeks after induction (Figure 4a). The extent of inflammation was strikingly ablated in *PAR-2*$^{-/-}$ mice, the magnitude being fourfold less than in the wild-type (P < 0.0001, two-way ANOVA), demonstrating the crucial role for this receptor in arthritis. *PAR-2*$^{+/-}$ mice showed an intermediate phenotype, the inflammatory response being significantly greater than that of *PAR-2*$^{-/-}$ mice (P < 0.0001, two-way ANOVA). Completely untreated wild-type animals had a 10.2% ± 2.4% (n = 7) increase in joint diameter by 28 days, which may explain the absence of reduction in joint diameter following the acute phase of inflammation in the *PAR-2*$^{-/-}$ group.

PAR-2 expression, as demonstrated by β-galactosidase activity in *PAR-2*$^{-/-}$ mice, is normally limited to small

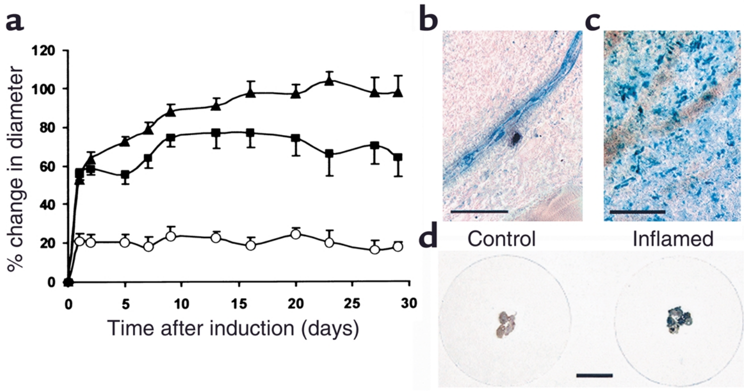

Figure 4
Chronic joint inflammation is inhibited by *PAR-2* gene disruption and PAR-2 is upregulated in inflamed tissues. (**a**) Comparison of the response to induction of adjuvant arthritis in *PAR-2*$^{+/+}$ mice (filled triangles), *PAR-2*$^{-/-}$ mice (open circles), and heterozygous mice (filled squares). An acute (24-hour) phase is followed by a progressive increase in joint diameter that reached a plateau by about 14 days in all but the *PAR-2*$^{-/-}$ group, which did not develop a chronic response. Data are presented as mean ± SEM; n = 6–8. (**b**) X-gal staining of normal synovial tissue in a *PAR-2*$^{-/-}$ mouse shows a rich density of staining for β-galactosidase activity limited to endothelial cells along the length of the arteriole. (**c**) Two weeks after induction of adjuvant monoarthritis in the *PAR-2*$^{-/-}$ mouse there is marked discrete extravascular cellular staining (scale bar: 50 μm for both **b** and **c**). (**d**) X-gal staining of inflamed synovial tissue excised from the knee joints of four *PAR-2*$^{-/-}$ mice shows very dense staining compared with uninflamed tissues from the contralateral knees (scale bar: 5 mm).

arterioles (Figure 4b and Figure 1d), but synovial samples taken 2–3 weeks after induction of inflammation showed staining of extravascular cells (Figure 4c); the density of staining was obvious even to the naked eye (Figure 4d). PAR-2 upregulation was also observed in surrounding muscle and skin, presumably from leakage of adjuvant to these tissues during induction, indicating that enhanced PAR-2 expression is associated with chronic inflammatory responses in many tissue types.

Histological examination of the knee joint at the conclusion of the experiment revealed severe arthritic changes in *PAR-2*$^{+/+}$ mice, characterized by cellular infiltration, synovial hyperplasia, and damage to articular cartilage (Figure 5a), with many mice scoring 9/9 (Table 1). In contrast, scores were substantially lower in *PAR-2*$^{-/-}$ mice (Figure 5b and Table 1), whose joints displayed similar histology to that of untreated animals (Figure 5c). Heterozygotes showed an intermediate degree of joint damage (Table 1); the difference between groups was significant (P < 0.0001, one-way ANOVA). In additional experiments, we confirmed that the 129/Ola strain, in whose ES cells the *PAR-2* null allele was created, did not confer resistance to inflammation in the *PAR-2*$^{-/-}$ mice as a consequence of a residual 129/Ola genetic background component still present at the backcross generation used. Specifically, the development of adjuvant arthritis in 129/Ola mice did not differ significantly (P = 0.4, two-way ANOVA) from that of wild-type C57BL/6 mice (see Figure 4a), with the 129/Ola strain showing a 98% increase in knee joint diameter at day 28.

Acute inflammatory responses to carrageenan/kaolin showed a significant (P = 0.0016, one-way ANOVA, n = 6–8) reduction in *PAR-2*$^{-/-}$ mice (18% ± 3.8% increase in knee joint diameter at 24 hours) compared with heterozygotes (25.6% ± 4.3% increase) and wild-type mice (40.4% ± 3.5% increase), but this effect was much less pronounced than was the ablation of the chronic inflammatory response.

Discussion

We demonstrate here a key role for PAR-2 in chronic inflammation, and present three lines of evidence to support our hypothesis. Chronic arthritis is ablated in PAR-2–deficient mice, identifying the essential role of this receptor in chronic inflammation. The second line of evidence is the long-lasting development of the cardinal signs of inflammation — joint swelling and vasodilatation — following application of PAR-2 agonists. Thirdly, we present evidence for substantial PAR-2 upregulation in chronically inflamed tissues.

Using the native peptide SLIGRL-NH_2 or a novel synthetic peptide, ASKH95, we demonstrate that direct activation of PAR-2 affects synovial vasculature, resulting in extravasation and inflammatory hyperemia. However, the nature of these effects differed considerably. ASKH95 produced a similar magnitude but longer-lasting vasodilatation than SLIGRL-NH_2, and also elicited greater joint swelling (72 hours vs. 24 hours) in *PAR-2*$^{+/+}$ mice, although the magnitude of the

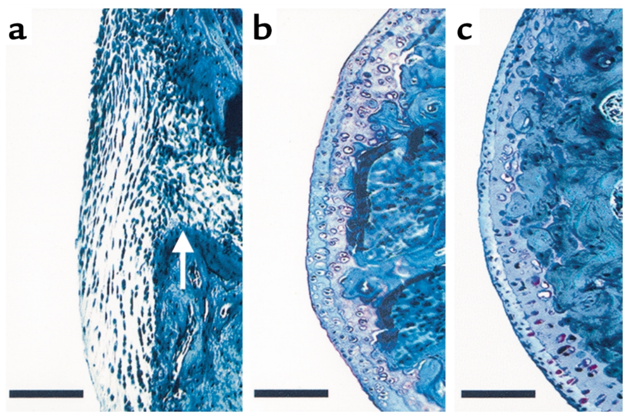

Figure 5
Histological evaluation of femoral cartilage integrity. (**a**) Thirty days after induction of adjuvant arthritis in a *PAR-2*$^{+/+}$ mouse, cartilage is completely replaced by pannus that has eroded cortical bone (arrow). (**b**) Thirty days after induction of adjuvant arthritis in a *PAR-2*$^{-/-}$ mouse. Note the intact appearance of cartilage, similar to that in the normal joint. (**c**) Normal (untreated) knee joint in a *PAR-2*$^{+/+}$ mouse. Sections stained with hematoxylin, safranin O, and fast green. Scale bar: 100 μm.

Table 1
Histological scoring of joint damage in mice with adjuvant-induced arthritis

	Cartilage	Hyperplasia	Infiltration	Total score
Untreated	0	0	0	0
PAR-2$^{+/+}$	2.8	3	3	8.8^{A,B}
PAR-2$^{+/–}$	1	2	2.7	5.7^{A}
PAR-2$^{–/–}$	0	0.2	0.5	0.7^{C}

$^{A}P < 0.001$ compared with untreated (control) joints (*PAR-2*$^{–/–}$ mice did not differ from untreated mice). $^{B}P < 0.001$ compared with both *PAR-2*$^{+/+}$ and *PAR-2*$^{+/–}$ mice. $^{C}P < 0.01$ compared with *PAR-2*$^{+/–}$ mice. Bonferroni post hoc testing. $n = 3–7$.

response over the initial 6 hours was not different. The longer duration of the effect of ASKH95 could be due either to persistent signaling of PAR-2 by this compound or a slow rate of metabolic degradation. We suggest the latter, since ASKH95 does not lead to prolonged Ca^{2+} signaling compared with SLIGKV-OH (our unpublished observations). The prolonged effect of ASKH95 is also unlikely to be due to differences in concentration of the agonists locally as they have similar molecular weights. However, ASKH95 is approximately 525 times more lipophilic than SLIGRL-NH_2, based on log *P* values of 0.56 and –2.14, respectively (calculated with Tsar software; Accelrys Inc., San Diego, California, USA), which would improve penetration and thus retention in the adipose-rich tissues of the synovium. Moreover, the substituted moiety (furoyl) in ASKH95 may reduce its metabolic degradation. The extended effect of ASKH95 in our experiments parallels the finding of Vergnolle et al. (16), who observed that *trans*-cinnamoyl-LIGRLO-NH_2 caused persistent edema and cellular infiltrate in the rat paw. Although the mechanism underlying the prolonged effect of ASKH95 remains uncertain, the kinetics of the responses to PAR-2 peptides is significant because it suggests that PAR-2 can be continually activated in vivo, despite evidence to suggest it is internalized rapidly when stimulated in vitro. The specificity of ASKH95 for PAR-2, which is expressed in the joint tissues of *PAR-2*$^{+/+}$ mice, was confirmed by its lack of vascular effects in *PAR-2*$^{–/–}$ mice. Moreover, the control peptide, ASKH115, had no effect in *PAR-2*$^{+/+}$ animals. Although derived from the human PAR-2 agonist SLIGKV, ASKH95 activates murine PAR-2. This was investigated using a secreted placental alkaline phosphatase assay (17) performed in NG108-15 cells expressing murine PAR-2; ASKH95 is fourfold more effective in these cells than is SLIGRL-NH_2. This is not surprising since human and murine PAR-2 receptors have been shown to respond comparably when activated by the human and murine PAR-2 agonist peptides SLIGKV and SLIGRL (9), indicating considerable interspecies cross-reactivity. Using the inositol turnover assay in NCTC2544 cells, we find ASKH95 to be about fivefold more effective than SLIGKV (our unpublished observation), paralleling the findings obtained in the murine PAR-2–expressing cells.

The most striking finding arose from the pivotal experiments in the chronic model of inflammation. This model is characterized by sustained joint swelling (Figure 4a), marked pannus formation, and cartilage erosion (Figure 5a). Although we used an aggressive model of arthritis causing extensive joint destruction in wild-type mice, signs of joint damage were virtually absent in PAR-2–deficient mice, indicating the absence of a key inflammatory component; this results in a failure of these animals to mount a chronic inflammatory response. Notably, although heterozygotes show an intermediate phenotype, the presence of even one *PAR-2* allele is sufficient to mount a substantial inflammatory response (~70% of wild-type; see Figure 4a). The fact that PAR-2 expression is powerfully upregulated in inflamed tissues, both articular and extra-articular, provides further evidence implicating PAR-2 in chronic inflammation and suggests that it is likely to play a central role in chronic inflammatory processes in many different tissues and organs. Indeed, it may be that PAR-2 is a key player in many chronic inflammatory processes, making it a very important target for future anti-inflammatory therapies. Although we were not able to investigate this directly, it is unlikely that the expression of β-galactosidase (the *lacZ* reporter gene product) could be responsible for the reduced inflammatory response in *PAR-2*$^{–/–}$ mice. There is no reported precedent for such an effect, and indeed, in a study by Yang et al. (18) in which the eotaxin gene was disrupted in mice with a *lacZ* reporter gene insertion, resulting in cell type–specific β-galactosidase expression, there was no reduced response to various inflammatory challenges in the lung.

An essential role for PAR-2 in chronic inflammation is unexpected, as previously PAR-2 had been shown to be significantly involved only in the mediation of neurogenic inflammation (1), which is relatively short-lived. Furthermore, Lindner and colleagues (19) have reported that although the inflammatory response to surgical trauma was delayed in PAR-2–deficient mice, this inhibition was not long-lasting. The substantial inhibition of adjuvant-induced arthritis we observed in the *PAR-2*$^{–/–}$ group, coupled with the failure of NK_1 receptor deletion to inhibit adjuvant arthritis (20), suggests that PAR-2 may mediate chronic joint inflammation by non-neurogenic mediators, perhaps via the cytokine cascade. Cytokines are known to play an important role in the pathogenesis of chronic inflammatory processes, and are targeted in current "biologic" therapies for rheumatoid arthritis. PAR-2 may be instrumental in cytokine pathways as its activation induces cytokine release from endothelial cells (21). Furthermore, PAR-2 is known to activate NF-κB (21) and stimulate prostanoid pathways (22), both of which are involved in mediating inflammation. Our findings provide the first evidence for PAR-2 orchestrating chronic inflammatory responses. However, the mechanisms which mediate this require further investigation. We have detected PAR-2 expression in fibroblasts derived from synovium of patients with rheumatoid arthritis (data not shown), suggesting that PAR-2 could prove an important future therapeutic lead for this condition. As PAR-2 is widely expressed and upregulated in many mammalian tissues, it may have a ubiquitous role in mediating chronic inflammation throughout the body, suggesting that our work has wide medical implications. Although PAR-2 antagonists are not currently available, our findings point toward development of such agents as an exciting avenue for future anti-inflammatory therapy.

Acknowledgments

We thank Laurence Cadalbert, Marion Drew, Gary Jackson, and David McMurdo for technical assistance, and Steve Campbell for advice and use of microscopy facilities. This work was supported by the Scottish Biomedical Foundation and Kowa Company Ltd. The Centre for Genome Research Gene Targeting Laboratory was supported by the Biotechnology and Biological Sciences Research Council.

1. Steinhoff, M., et al. 2000. Agonists of proteinase-activated receptor-2 induce inflammation by a neurogenic mechanism. *Nat. Med.* **6**:151–158.
2. Vergnolle, N., et al. 2001. Proteinase-activated receptor-2 and hyperalgesia: a novel pain pathway. *Nat. Med.* **7**:821–826.
3. Damiano, B.P., D'Andrea, M.R., de Garavilla, L., Cheung, W.M., and Andrade-Gordon, P. 1999. Increased expression of protease activated receptor-2 (PAR2) in balloon-injured rat carotid artery. *Thromb. Haemost.* **81**:808–814.
4. Nehls, M., et al. 1996. Two genetically separable steps in the differentiation of thymic epithelium. *Science.* **272**:886–889.
5. Smith, A.G. 1991. Culture and differentiation of embryonic stem cells. *J. Tissue Cult. Methods.* **13**:89–94.
6. Bradley, A. 1987. Production and analysis of chimaeric mice. In *Teratocarcinoma and embryo derived stem cells: a practical approach*. E.J. Robertson, editor. IRL Press. Oxford, United Kingdom. 113–151.
7. Bertog, M., et al. 1999. Basolateral proteinase-activated receptor (PAR-2) induces chloride secretion in M-1 mouse renal cortical collecting duct cells. *J. Physiol.* **521**:3–17.
8. Mountford, P., et al. 1994. Dicistronic targeting constructs: reporters and modifiers of mammalian gene expression. *Proc. Natl. Acad. Sci. USA.* **91**:4303–4307.
9. Blackhart, B.D., et al. 1996. Ligand cross-reactivity within the protease-activated receptor family. *J. Biol. Chem.* **271**:16466–16471.
10. Maryanoff, B.E., et al. 2001. Protease-activated receptor-2 (PAR-2): structure-function study of receptor activation by diverse peptides related to tethered-ligand epitopes. *Arch. Biochem. Biophys.* **386**:195–204.
11. Kanke, T., et al. 2001. Proteinase-activated receptor-2-mediated activation of stress-activated protein kinases and inhibitory κB kinases in NCTC 2544 keratinocytes. *J. Biol. Chem.* **276**:31657–31666.
12. Plevin, R., Kellock, N.A., Wakelam, M.J.O., and Wadsworth, R. 1994. Regulation by hypoxia of endothelin-1-stimulated phospholipase D activity in sheep pulmonary artery cultured smooth muscle cells. *Br. J. Pharmacol.* **112**:311–315.
13. Ramage, R., et al. 1999. Comparative studies of Nsc and Fmoc as N(alpha)-protecting groups for SPPS. *J. Pept. Sci.* **5**:195–200.
14. Lam, F.Y., and Ferrell, W.R. 1993. Acute inflammation in the rat knee joint attenuates sympathetic vasoconstriction but enhances neuropeptide-mediated vasodilatation assessed by laser Doppler perfusion imaging. *Neuroscience.* **52**:443–449.
15. Damiano, B.P., et al. 1999. Cardiovascular responses mediated by protease-activated receptor-2 (PAR-2) and thrombin receptor (PAR-1) are distinguished in mice deficient in PAR-2 or PAR-1. *J. Pharmacol. Exp. Ther.* **288**:671–678.
16. Vergnolle, N., Hollenberg, M.D., Sharkey, K.A., and Wallace, J.L. 1999. Characterization of the inflammatory response to proteinase-activated receptor-2 (PAR_2)-activating peptides in the rat paw. *Br. J. Pharmacol.* **127**:1083–1090.
17. Berger, J., Hauber, J., Hauber, R., Geiger, R., and Cullen, B.R. 1988. Secreted placental alkaline phosphatase: a powerful new quantitative indicator of gene expression in eukaryotic cells. *Gene.* **66**:1–10.
18. Yang, Y., Loy, J., Ryseck, R.P., Carrasco, D., and Bravo, R. 1998. Antigen-induced eosinophilic lung inflammation develops in mice deficient in chemokine eotaxin. *Blood.* **92**:3912–3923.
19. Lindner, J.R., et al. 2000. Delayed onset of inflammation in protease-activated receptor-2-deficient mice. *J. Immunol.* **165**:6504–6510.
20. De Felipe, C., et al. 1998. Altered nociception, analgesia and aggression in mice lacking the receptor for substance P. *Nature.* **392**:394–397.
21. Shpacovitch, V.M., et al. 2002. Agonists of proteinase-activated receptor 2 induce cytokine release and activation of nuclear transcription factor kappaB in human dermal microvascular endothelial cells. *J. Invest. Dermatol.* **118**:380–385.
22. Asokananthan, N., et al. 2002. Activation of protease-activated receptor (PAR)-1, PAR-2 and PAR-4 stimulate IL-6, IL-8 and prostaglandin E(2) release from human respiratory epithelial cells. *J. Immunol.* **168**:3577–3585.